

Nonlinear Soil Response in the Vicinity of the Van Norman Complex Following the 1994 Northridge, California, Earthquake

by Giovanna Cultrera, David M. Boore, William B. Joyner, and Christopher M. Dietel

Abstract Ground-motion recordings obtained at the Van Norman Complex from the 1994 Northridge, California, mainshock and its aftershocks constitute an excellent data set for the analysis of soil response as a function of ground-motion amplitude. We searched for nonlinear response by comparing the Fourier spectral ratios of two pairs of sites for ground motions of different levels, using data from permanent strong-motion recorders and from specially deployed portable instruments. We also compared the amplitude dependence of the observed ratios with the amplitude dependence of the theoretical ratios obtained from 1-D linear and 1-D equivalent-linear transfer functions, using recently published borehole velocity profiles at the sites to provide the low-strain material properties. One pair of sites was at the Jensen Filtration Plant (JFP); the other pair was the Rinaldi Receiving Station (RIN) and the Los Angeles Dam (LAD). Most of the analysis was concentrated on the motions at the Jensen sites. Portable seismometers were installed at the JFP to see if the motions inside the structures housing the strong-motion recorders differed from nearby free-field motions. We recorded seven small earthquakes and found that the high-frequency, low-amplitude motions in the administration building were about 0.3 of those outside the building. This means that the lack of high frequencies on the strong-motion recordings in the administration building relative to the generator building is not due solely to nonlinear soil effects. After taking into account the effects of the buildings, however, analysis of the suite of strong- and weak-motion recordings indicates that nonlinearity occurred at the JFP. As predicted by equivalent-linear analysis, the largest events (the mainshock and the 20 March 1994 aftershock) show a significant deamplification of the high-frequency motion relative to the weak motions from aftershocks occurring many months after the mainshock. The weak-motion aftershocks recorded within 12 hours of the mainshock, however, show a relative deamplification similar to that in the mainshock. The soil behavior may be a consequence of a pore pressure buildup during large-amplitude motion that was not dissipated until sometime later. The motions at (RIN) and (LAD) are from free-field sites. The comparison among spectral ratios of the mainshock, weak-motion coda waves of the mainshock, and an aftershock within ten minutes of the mainshock indicate that some nonlinearity occurred, presumably at (RIN) because it is the softer site. The spectral ratio for the mainshock is between that calculated for pure linear response and that calculated from the equivalent-linear method, using commonly used modulus reduction and damping ratio curves. In contrast to the Jensen sites, the ratio of motions soon after the high-amplitude portion of the mainshock differs from the ratio of the mainshock motions, indicating the mechanical properties of the soil returned to the low-strain values as the high-amplitude motion ended. This may indicate a type of nonlinear soil response different from that affecting motion at the Jensen administration building.

Introduction

The seismic response of near surface soils has usually been modeled by seismologists on the assumption that the

stress-strain relationship of such materials is linear. Geotechnical laboratory measurements, however, indicate that

soils behave in a nonlinear fashion at the strain levels corresponding to damaging ground motions. The laboratory measurements show a reduction of shear modulus and an increase in damping as the strain level increases. The effect on seismic waves would be an increase in damping and a decrease in propagation velocity, with consequent reduction in high-frequency amplitudes and shifts to lower frequencies of the spectral resonant peaks of the soil deposit. There are reasons, however, for concern about the degree to which the laboratory measurements are representative of the behavior of the soil *in situ* (EPRI, 1993, Appendix 7A). It is important, therefore, to verify the laboratory-based predictions with actual strong-motion data. It is necessary to evaluate not only whether nonlinear behavior occurs, but also more specifically, the degree of nonlinearity, the frequency range and amplitude levels at which it occurs, and the materials in which it occurs. In our subsequent discussion of nonlinear soil response, it will be useful to distinguish between two forms of nonlinear soil response. In one form, the modulus decreases and the damping increases as the amplitude increases, returning to their low-strain values as soon as the high-amplitude motion ends. In the other form, particularly common in loose sands, the pore pressure may build up gradually as a consequence of repeated cycles of shear deformation. As the pore pressure builds up, the modulus decreases, the damping increases, and the changes may persist for hours after the motion ceases. These two forms of nonlinear soil behavior may occur in combination with each other.

Until recently, only very limited strong-motion data were available for evaluating soil nonlinearity at high strains. Many recordings of strong motion, however, have been collected from recent large earthquakes (1985 Michoacan, 1989 Loma Prieta, 1994 Northridge, 1995 Hyogo-ken Nanbu), creating new opportunities to evaluate the issue of soil nonlinearity. In particular, for the Northridge earthquake, a systematic nonlinear response at soil sites has been found by several groups of researchers. The conclusion that soil nonlinearity was present was arrived at in a number of ways, but in all cases the basic evidence was that the motions at soil sites subjected to strong shaking was smaller than expected. Trifunac and Todorovska (1996) found that non-parametric attenuation functions fit to mainshock peak accelerations at soil sites resembled those from rock sites at distances beyond about 20 km but, unlike rock sites, leveled off at closer distances. Field *et al.* (1997, 1998) and Hartzell (1998) derived spectral amplification factors for soil sites relative to a selected set of rock sites after removing distance dependence; the amplifications from recordings of the mainshock in the San Fernando Valley were significantly less than found for much weaker-motion aftershocks recorded on a set of portable recorders. Beresnev *et al.* (1998a) and Su *et al.* (1998) also used weak-motion amplification functions but applied them to theoretical rock-motion simulations to predict soil motions; their simulations fit the rock motions but overpredict the soil motions (as did studies by Field *et al.*, 1997, 1998). Beresnev *et al.* (1998b) studied spectral ratios for soil and rock stations separated by 3.2 and 4.8 km;

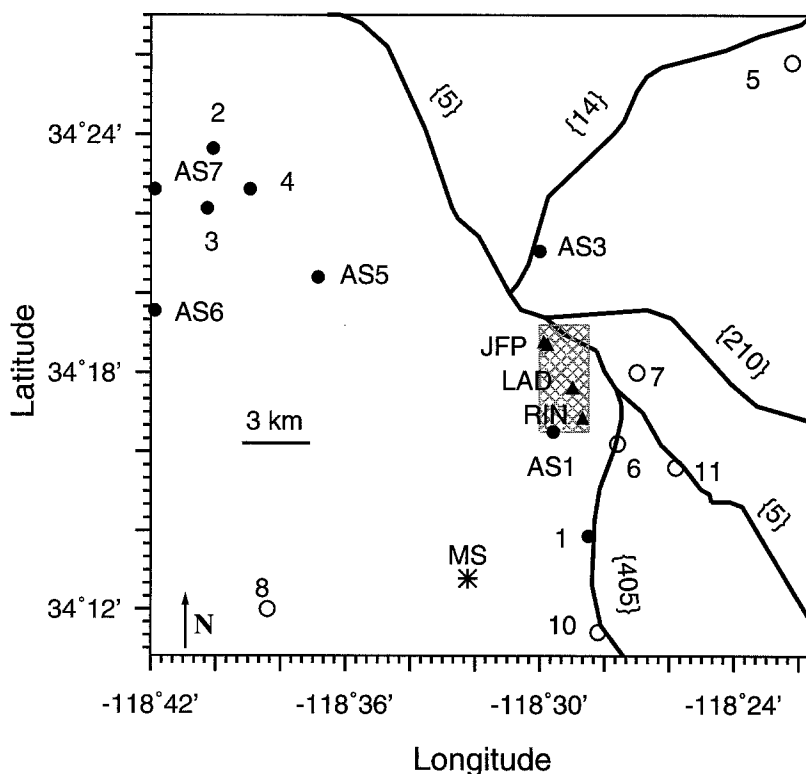


Figure 1. Map showing the epicenters of the events used in our study. The event numbers are keyed to event information in Table 3 (event 9 is located outside of the area shown in the figure). Events recorded on permanent accelerographs and GEOS portable instruments are indicated by filled and empty circles, respectively. The triangles indicate the positions of the SMA-1 recording stations: LAD, RIN, and the two sites (JAB and JGB) at the Jensen Filtration Plant (JFP). The numbers in curly brackets are the route numbers of major highways. The area within the shaded rectangle is shown in Figure 2.

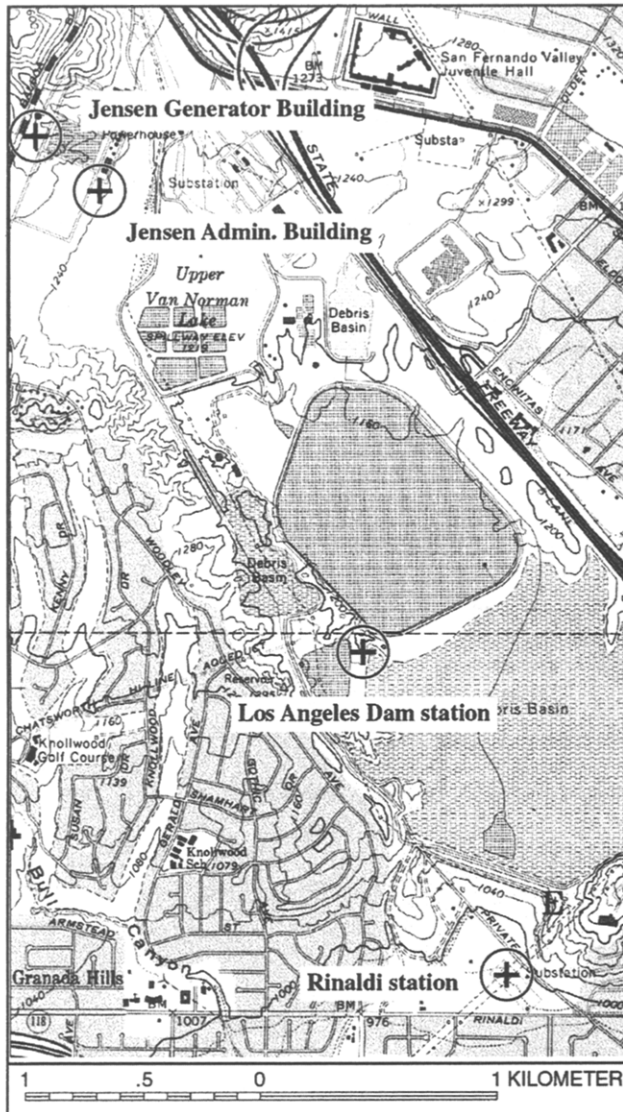


Figure 2. Topographic map (San Fernando Quad-range) with the position of the four SMA-1 stations in the Van Norman Complex (this is the region indicated by the shaded rectangle in Figure 1).

they found a shift in the frequency of spectral peaks for the mainshock, aftershocks, and the 1987 Whittier Narrows earthquake that are consistent with nonlinear soil response.

As in many of the studies just mentioned, we also used spectral ratios to look for nonlinear soil response. We feel that using spectral ratios is the simplest and most direct way to demonstrate soil nonlinearity. Our study, however, differs in a number of essential ways from other studies of nonlinear soil response during the 1994 Northridge, California, earthquake:

- We used two pairs of stations in the Van Norman Complex (VNC), which were situated in an area subjected to some of the strongest shaking produced by the earthquake.

- Our station pairs are much closer together (0.3 and 1.5 km) than in the other studies.
- Shear-velocity and low-strain damping values are available from borehole logging at each site that we used in our analysis.
- Spectral ratios for a very wide range of ground-motion amplitudes were used in our study.
- We deployed digital seismic recorders to define the effect of the buildings on the strong-motion recordings obtained from the permanent stations located within the buildings.
- We compared the observed amplitude dependence of the spectral ratios with that predicted from conventional engineering practice (using SHAKE91). In the predicted response we used low-strain damping obtained from the borehole data, and we included the response of the reference site (something that is rarely done in site response analysis) by deconvolving the observed reference-site motion to a depth at which we judged the material properties underlying the sites to be the same. In the subsequent sections, we describe the stations and the data recorded, discuss the methods of data analysis, and finally show the recorded and theoretically predicted relative site response at the two pairs of stations for different events.

Data

The VNC includes important engineering facilities owned and operated by the Los Angeles Department of Water and Power (LADWP) and the Metropolitan Water District of Southern California (MWD). It is located in the northern San Fernando valley (Figs. 1, 2) and supplies a large amount of water and power to the city of Los Angeles. Because of its importance and position close to active faults, the VNC has been instrumented with strong-motion accelerographs since the 1971 San Fernando earthquake. Figure 1 shows the location of the VNC and the epicentral locations of the 17 January 1994 Northridge mainshock and the aftershocks used in this study. The mainshock occurred 11-km southwest and ruptured updip toward the VNC, such that the VNC is above a portion of the rupture surface (Trifunac *et al.*, 1994; Scientists, 1994; Wald *et al.*, 1996). Field observations revealed sand boils, both at the north end of the VNC (Bardet and Davis, 1996c) and close to the Jensen Filtration Plant (JFP) (Stewart *et al.*, 1996), and evidence of liquefaction at the Lower San Fernando Dam, located between the Los Angeles Dam (LAD) and the Rinaldi Receiving Station (RIN) (Bardet and Davis, 1996b). Some of the strongest shaking recorded during the mainshock occurred in this region (e.g., Bardet and Davis, 1996a). The large ground motions make this region an ideal one for looking for nonlinear soil response.

The position of the four sites we analyzed in this study are shown in Figure 2, with station information contained in Table 1. Two of the stations are in the JFP, and the other pair are the stations at the west abutment of LAD and RIN.

Table 1
Location of Recording Stations

Station	Code	Instrument	Owner/Agency	Lat.* (deg)	Long.* (deg)
Admin. building	JAB	SMA-1/GEOS	MWD-USGS	34.31151	-118.49665
Admin. free-field	JABF	GEOS	USGS	34.31088	-118.49654
Generator building	JGB	SMA-1/GEOS	MWD-USGS	34.31299	-118.49884
Generator free-field	JGBF	GEOS	USGS	34.31309	-118.49906
LA Dam west abutment	LAD	SMA-1	LADWP	34.281	-118.478
Rinaldi receiving station	RIN	SMA-1	LADWP	34.294	-118.483

*Coordinates at Jensen Filtration Plant using a handheld precision GPS unit with accuracy better than 4m.

Borehole measurements close to these sites (Figure 4 and Table 2) provided shear-wave velocity profiles to depths of about 90 m and soil damping factors for low strain (Gibbs *et al.*, 1996; J. Gibbs, personal comm., 1997). Details about the earthquake locations and magnitudes, as well as information about the recorded motions, are given in Table 3.

Records of the mainshock and some aftershocks are also available at several other sites in the vicinity (in particular, the Sylmar Converter Station about 0.7 km east of the Jensen administration building). We did not use records from these other sites in this article because it was not clear with which recordings they should be compared. The two stations at the JFP and the stations RIN and LAD provided a more closely spaced pair of recordings on different materials than if we had compared recordings at the Sylmar Converter Station with one of the Jensen stations or with the LAD station.

Jensen Filtration Plant: Stations and Recordings

Our main focus in this study is on recordings obtained from two triggered, analog strong-motion accelerographs (SMA-1) at the JFP [the stations are owned by the MWD but are maintained by the U.S. Geological Survey (USGS)]. These accelerographs are located in the administration building (JAB) and the generator building (JGB) at JFP (Figure 3). The accelerograph at JAB is located about 3–4 m below ground level in a corner of the basement of a 28 × 60 meter two-story building, and the instrument at JGB is in the ground floor of a 10 × 10 × 3.6 m concrete block structure, with a concrete slab foundation over fill (D. Dean, personal comm., 1998). The JAB and JGB sites are 260 m apart but situated on very different soils. Borehole measurements close to JAB and JGB (within 57 and 31 meters, respectively) indicate that JAB and JGB are sited on about 14 m of engineered fill and alluvium and 3 m of engineered fill, respectively (Gibbs *et al.*, 1996; J. Tinsley, personal comm., 1998). At both sites, the Holocene fill and alluvium are underlain by the upper member of the Plio-Pleistocene Saugus Formation. The material under JAB has a significantly lower shear-wave velocity than under the JGB for depths less than about 60 m (Figure 4 and Table 2). However, the average low-strain shear-wave damping ratio D (related to quality factor Q_s by $D = 100/(2Q_s)$, with D in percent) under each site is similar ($D = 3.6\%$ and $D = 3.0\%$ for JAB and JGB, respectively; see Table 2).

Table 2
Borehole Information

Borehole	Latitude (deg)	Longitude (deg)	D^* (%)	depth range (m)	V_{30}^\dagger (m/sec)
JAB	34.31100	-118.49667	3.6 + 0.2	10–90	375
JGB	34.31311	-118.49914	3.0 + 0.2	10–90	569
LAD	34.2931	-118.4839	7.8 + 3.8	10–89	647
RIN	34.2810	-118.4771	1.1 + 0.3	15–70	336

* D (damping ratio in percent = $100/(2Q_s)$) determined by J. Gibbs from analysis of downhole recordings (written commun., 1997)

† shear velocity averaged over the upper 30 m

Although the boreholes are displaced some distance from the strong-motion accelerograph sites (Figure 3), consideration of the local geology, along with borings made following the 1971 San Fernando earthquake (O'Rourke *et al.*, 1992), suggests that the borehole velocities are representative of the velocities beneath the recording sites (J. Tinsley, personal comm., 1998).

The low-velocity zone shown under the borehole near JAB (Figure 4) corresponds to fluvial terrace deposits. Liquefaction following the 1971 San Fernando earthquake (and possibly following the 1994 Northridge earthquake) occurred within these terrace deposits. Furthermore, as we discuss later, nonlinear calculations show that these terrace deposits are of fundamental importance in the nonlinear response of the site.

The accelerographs at JAB and JGB that were triggered by the mainshock continued operating for about 146 sec and recorded a number of aftershocks on the same film. The same accelerographs also recorded a number of aftershocks hours to years after the mainshock. The mainshock time series were obtained from the USGS web site (<http://nsmf.wr.usgs.gov/>); we digitized the aftershocks AS1, AS2, AS3, AS4, 1, 2, 3, and 4 (Table 3) from the original film records with standard USGS procedures (a 600 dpi flatbed scanner and trace-following software from Kinometrics). The time series for aftershocks AS6 and AS7 were obtained from independent digitizing of the film records by the University of Southern California (USC; data provided by M. Todorovska).

Immediately after the mainshock, digital aftershock recorders were deployed at JGB by the USGS (G. Glassmoyer,

Table 3
Events Used in this Study (SCEC data base) and PGV and PGA of Recordings at the Stations

Event	Date (yy/mm/dd)	Origin Time (hh:mm:ss)	M	Lat. (deg)	Long. (deg)	Depth (Km)	PGV (cm/s)#		PGA (g)**			
							JAB	JGB	JAB	coda	JGB	coda
MS*	94/01/17	12:30:55.39	6.7	34.213	-118.537	18.4	98.3	69.3	0.498	0.116	0.755	0.123
AS1†	94/01/17	12:31:58.12	5.9	34.275	-118.493	6	5.4	6.4	0.08	0.017	0.131	0.022
AS2	94/01/17	12:32:41					0.7	1.0	0.019	—	0.037	—
AS3	94/01/17	12:32:54.53	3.3	34.351	-118.5	10	2.9	2.7	0.039	0.011	0.069	0.016
AS4	94/01/17	12:33:15					0.7	0.4	0.012	—	0.016	—
AS5‡	94/01/17	12:40:36.12	5.1	34.340	-118.614	6.0						
AS6	94/01/17	23:33:30.69	5.5	34.326	-118.698	9.8	1.3	1.4	0.021	—	0.027	—
AS7	94/01/18	00:43:08.89	5.2	34.377	-118.698	11.3	3.3	2.8	0.050		0.065	
1§	94/03/20	21:20:12.26	5.3	34.231	-118.475	15	18.4	16.9	0.238	0.024	0.225	0.020
2	95/06/26	08:40:28.94	5	34.394	-118.668	13.3	1.7	1.8	0.037	0.015	0.032	0.013
3	97/04/26	10:37:30.66	5.1	34.369	-118.671	16.5	—	—	0.033	—	0.027	—
4	97/04/27	11:09:28.38	4.9	34.377	-118.649	15.2	—	—	0.016	—	0.013	—
5	97/11/27	10:43:02.5	2.4	34.43	-118.37	6.7	0.0035	0.0044	—	—	—	—
6	97/11/29	00:12:29.8	1.6	34.27	-118.46	10.8	0.013	0.011	—	—	—	—
7	97/12/04	09:16:25.5	2.6	34.30	-118.45	8.0	0.079	0.13	—	—	—	—
8	98/01/04	09:11:45.1	3.3	34.20	-118.64	3.5	0.026	0.019	—	—	—	—
9	98/01/05	18:14:06.5	4.3	33.95	-117.71	11.5	0.073	0.094	—	—	—	—
10	98/01/12	06:36:24.9	3.4	34.19	-118.47	11.3	0.075	0.1	—	—	—	—
11	98/01/15	22:54:08.1	3.0	34.26	-118.43	10.6	0.088	0.15	—	—	—	—

Event	LAD	RIN	LAD	coda	RIN	coda
MS	58.8	114.3	0.369	0.068	0.640	0.149
AS5	8.4	3.4	0.110	—	0.055	—

*Northridge mainshock.

†Events AS1, 2, 3, 4 are the aftershocks within 2 minutes after the mainshock: AS1 and AS3 locations from CNSS (Council of the National Seismic System) catalog; AS2 and AS4 were not located by the southern California seismic network. Coda waves for events AS2 and AS4 were not used.

‡Events AS5, 6, 7 were processed by University of Southern California; locations from CNSS catalog.

§Numbers are used to identify events in Figure 1.

||Magnitudes are M_L , except for the mainshock (M_W) and AS3 (coda magnitude).

#Geometric mean of horizontal peak ground velocities determined from uncorrected time series for events 5 to 11 (GEOS recordings) and from corrected time series for events AS5, 6, 7. Velocities of all other events obtained by integration of filtered ground accelerations.

**Geometric mean of horizontal peak ground accelerations; GEOS recordings not processed to yield PGA.

personal comm., 1998) and near JAB by the University of California at Santa Barbara (J. Steidl, personal comm., 1997). These recorders were in the field for several weeks to several months. Unfortunately, the instrument at JAB was not colocated at the strong-motion accelerograph; it was located at least 30 m outside the southeast corner of the building. As discussed below, we have good evidence that the motions from the accelerograph at JAB are not equivalent to a free-field site outside of the building, and because we wish to compare strong and weak motions at JAB, the aftershock deployments immediately following the mainshock did not help us. Fortunately, we could obtain records for a wide range of amplitudes from the accelerographs themselves.

As a result of our initial analysis of the accelerograph data, we suspected that the recording of the mainshock at JAB was significantly affected by the response of the structure in which the recorder is located. We confirmed that this was the case by using a special deployment of portable recorders in 1997–1998 to obtain ground motion inside and outside the buildings in which the permanent accelerographs are located. We used four General Earthquake Observation System (GEOS) velocity digital recorders (see Borchardt *et*

al., 1985), which we placed at sites next to the SMA-1 accelerographs in the two buildings and at free-field sites close to the buildings. The locations are shown in Figure 3.

Rinaldi Receiving Station and Los Angeles Dam: Stations and Recordings

The other pair of stations studied in this article are RIN and LAD; the two sites are 1.5 km apart. These are free-field sites; the instruments are housed in small shelters and are attached to isolated concrete slabs that are firmly anchored to the ground, away from the influence of any building structures (Bardet and Davis, 1996a). The instruments are operated by LADWP and the recordings of the mainshock were digitized by Lindvall-Richter-Benuska Associates (1994). We also used time series for an aftershock (AS5 in Table 3) provided by M. Todorovska at USC.

Station RIN is located at the southern tip of the VNC, on relatively fine-textured surficial alluvium deposits (the average velocity to 30 m, V_{30} , is 336 m/sec, and the damping $D = 1.1\%$). The mainshock accelerogram at this station provided the largest velocity ever instrumentally recorded (Heaton *et al.*, 1995; Wang *et al.*, 1996).

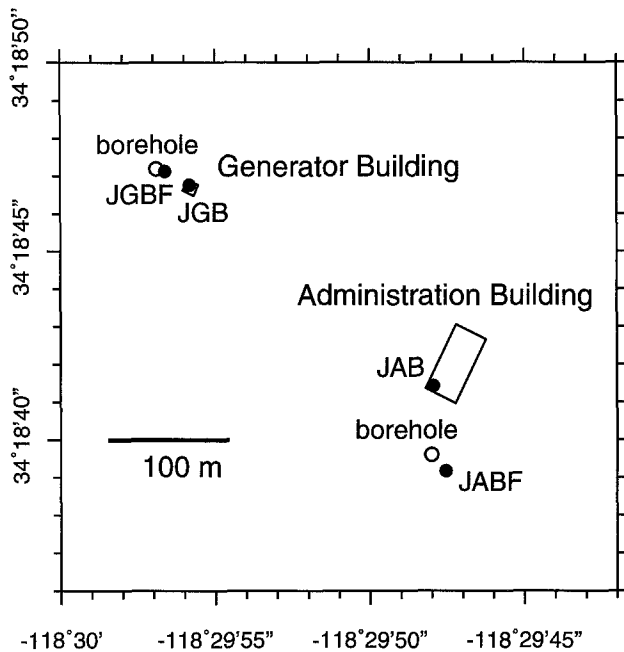


Figure 3. Map of the Jensen Filtration Plant, showing an approximation of the building outlines and the locations of the accelerographs (JAB and JGB), the boreholes, and the portable GEOS units (JABF, JGBF).

Station LAD is located on the ground surface at the west abutment of the dam. Peak ground accelerations recorded at the dam are lower than elsewhere in the VNC. The borehole investigation at 35 m from the accelerograph showed that the site is a rock site ($V_{30} = 647$ m/sec) within the lower (Sunshine Ranch) member of the Saugus Formation; the measured shear-wave velocities are higher than those measured in the younger Saugus Formation sites. Using the methods of Gibbs *et al.* (1994), Gibbs (personal comm., 1997) used the borehole data to derive a low-strain damping of $D = 7.8 \pm 3.8\%$ ($Q = 6.4$), averaged over a depth of 10 to 89 m (Table 2). This may seem like an unusually large amount of damping for a rock site, but the large value is supported by the spectral decay parameter κ that we determined by fitting a straight line to a log-linear plot of the Fourier spectrum of the mainshock record at each station (see Anderson and Hough, 1984). We found $\kappa = 0.063$ sec at the rock site (LAD), which is close to that at the soil site (RIN, $\kappa = 0.059$ sec). The value of κ is determined over a greater depth range than is penetrated by the boreholes, so we do not expect a one-to-one correlation with the damping values determined from the borehole measurements. The values of both κ and D , however, are greater for the rock site (LAD) than for the soil site (RIN).

As discussed by Lindvall-Richter-Benuska Associates (1994), the digital acceleration time series we used for RIN was corrected to account for an apparently short-duration stall of the film transport mechanism. Recently, Trifunac *et al.* (1998) corrected the acceleration time series for many

other but shorter stalls. The acceleration, velocity, and displacement waveforms, as well as the undamped response spectra, for the newly corrected acceleration time series are very similar to those from the time series we used in this article, and therefore we did not redo the analysis using the newly corrected time series.

Method of Data Analysis

The heart of our analysis is a comparison of spectral ratios of the motions at nearby sites for different amplitudes of the shaking at the reference site, the site that provides motions for the denominator of the spectral ratios. The spectral ratio method is based on the assumption that a seismic signal is represented by the convolution of functions describing source, path, site effect, and instrumental response. If the distance between the stations is much smaller than their hypocentral distances, the source and path effects on the records are nearly identical. In our case, the instruments are essentially identical, and therefore any differences in the records can largely be attributed to site effects, with minor variations due to differing incidence angles and the heterogeneity of the medium. The distance between JAB and JGB (0.3 km) is small enough that the spectral ratio most likely eliminates all but the differences in ground motion due to variations in the local geologic materials; this is less true for RIN and LAD, which are separated by 1.5 km. For both pairs of sites, we chose the site underlain by the higher velocity materials as the reference site. These are JGB and LAD.

We computed the spectral ratios as follows. We first conditioned the time series by removing a linear trend from the uncorrected SMA-1 data (this was not required for the GEOS data), windowing the time series to extract the *S*-wave motion (or in some cases, a specified portion of the signal coda), and padding with zeros in order to ensure the same frequency spacing (0.1 Hz) for all analyses. We tried several window lengths to make sure that the results were not sensitive to the choice of window length. After windowing, we computed spectral amplitudes of the horizontal motions from the Fourier transforms of the two horizontal components by summing the squared amplitude spectra, smoothing the value of the sum with an operator that returns the median of the amplitude in 0.5 Hz bins (using the MATLAB function `medfilt1`), and taking the square roots of the smoothed spectra. The ratios were computed from the smoothed spectra, and to facilitate the comparison for the various events, emphasizing the overall trend and eliminating large fluctuations, the ratios were smoothed using a 1 Hz median operator. We did tests to insure that the results are not sensitive to the choice of smoothing operators.

The decision to combine the horizontal components instead of rotating them into longitudinal and transverse directions was motivated by the difficulty of determining a single point source from which the motions originated; the near-fault recordings of the Northridge 1994 mainshock are comprised of three successive *S*-wave arrivals coming from

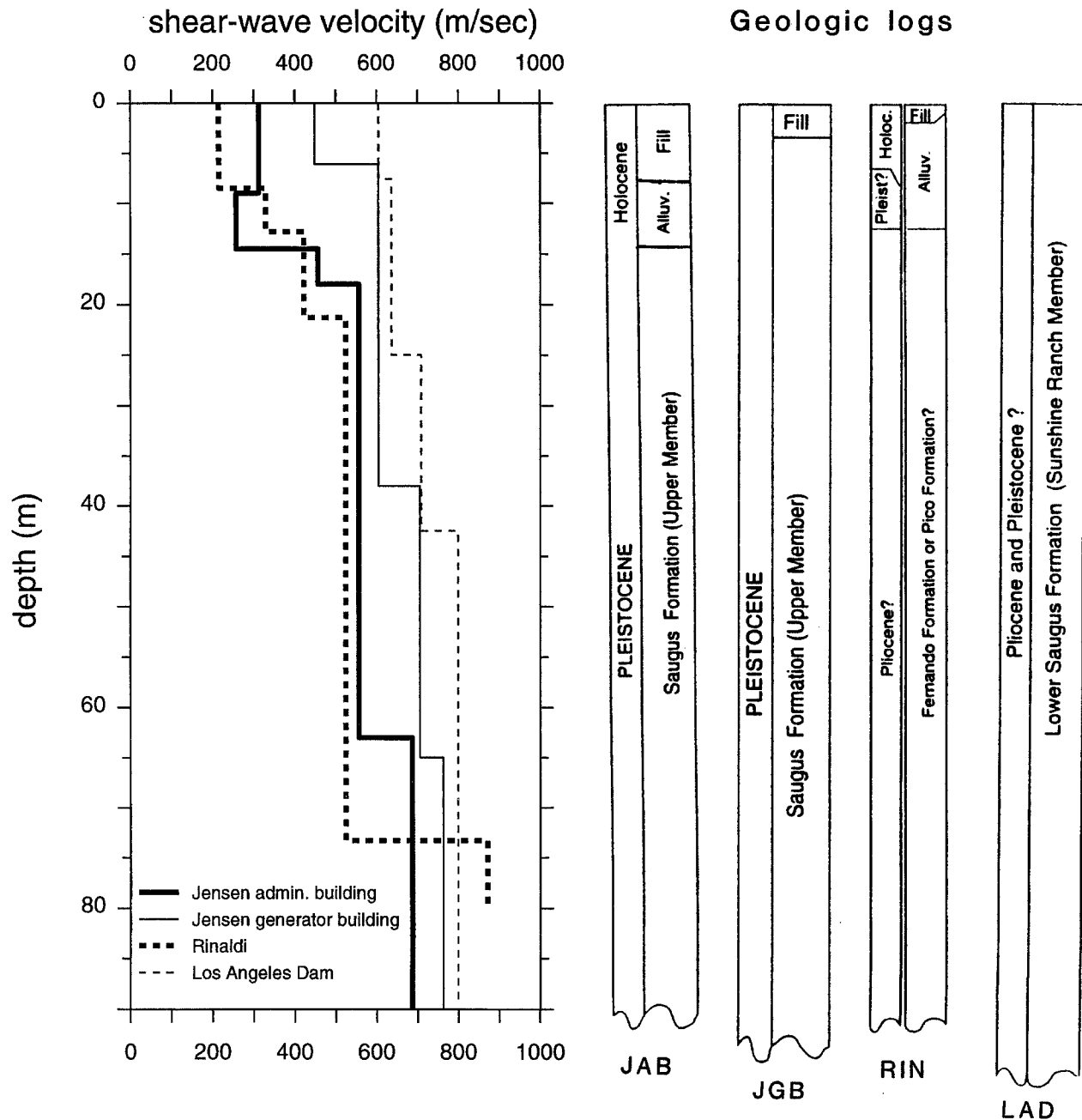


Figure 4. Shear-wave velocity profiles computed at four sites close to the recording stations (JAB, JGB, RIN, and LAD). Simplified geologic logs are shown for correlation with velocities, giving the probable geologic age and the correlation with regionally mapped geologic units (from Gibbs *et al.* 1996).

different positions on the fault (Wald *et al.*, 1996). In addition, the locations of some of the aftershocks occurring within a few minutes of the mainshock have not been determined.

We restricted our study to frequencies between 1 and 10 Hz, a frequency range of importance to civil engineering. We performed a signal-to-noise analysis to show that the windowed records are reliable at least from 1 to 10 Hz, and we simulated the analog-to-digital process to verify that dig-

itizing the low-amplitude film records did not alter the spectral estimates above 1 Hz. We did the latter by simulating the time series of a small earthquake, converting the amplitudes to pixel units, truncating to the nearest integer values, and then comparing the Fourier amplitude spectrum of the "digitized" record with the spectrum of the original record. The differences were not significant in the 1–10 Hz frequency range. We also processed one of the fixed traces adjacent to the smallest aftershock (AS4) as if it were a data

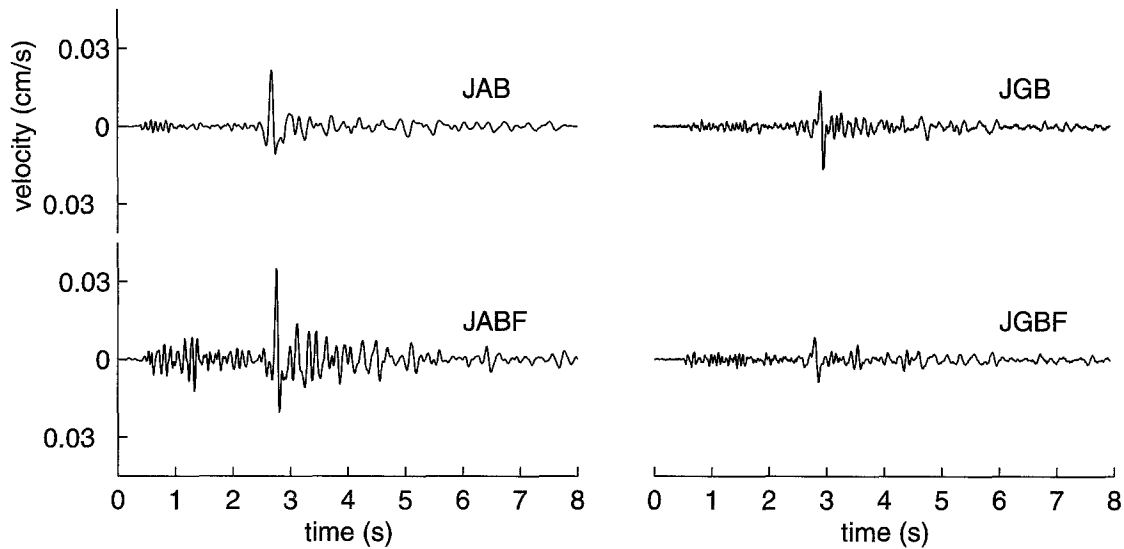


Figure 5. North component velocity of the 29 November 1997 event recorded by the four GEOS velocity digital recorders inside and outside the Jensen administration and generator buildings (JAB, JABF and JGB, JGBF).

trace and found that the Fourier spectrum from this fixed trace was at least a factor of 8 times smaller than the Fourier spectrum from the aftershock over the 1–10 Hz frequency range. We conclude that digitizing and processing noise is much smaller than the signal between 1 to 10 Hz, even for the smallest motions studied in this article.

JGB), and at free-field sites, close to the borehole locations (JABF, JGBF). The relative locations of the building sites and free-field sites are shown in Figure 3. The instruments recorded several events whose peak ground velocity (PGV) at JGB ranged from 0.005 to 0.15 cm/sec (Table 3). Figure

Analysis of Data from the Jensen Filtration Plant

The two permanent accelerograph stations at the JFP constitute an ideal site-response experiment: they are situated on very different soils and yet are close to one another (thereby making it likely that they have the same source and path effects), and they provided many records of different-size earthquakes. Unfortunately, both of the SMA-1 accelerographs are housed in buildings, and as we will show, there is a significant effect of the buildings on the records. We first discuss the results of our experiment for assessing the importance of the structures on the recordings. We then compare the spectral ratios of data obtained from the permanent accelerographs, after correcting the ratios for the effects of the structures. The data include recordings of the mainshock, aftershocks that occurred minutes to years after the mainshock, coda waves of the mainshock, and a few coda waves of the aftershocks. The aftershocks have been divided into two groups: those that occurred months to years after the mainshock, and aftershocks that occurred within a half day of the mainshock.

Effect of the Buildings on the Recordings (GEOS Data)

In order to investigate the influence of the structures on the seismic motion, we set up GEOS recording stations in the buildings, close to the SMA-1 accelerographs (JAB,

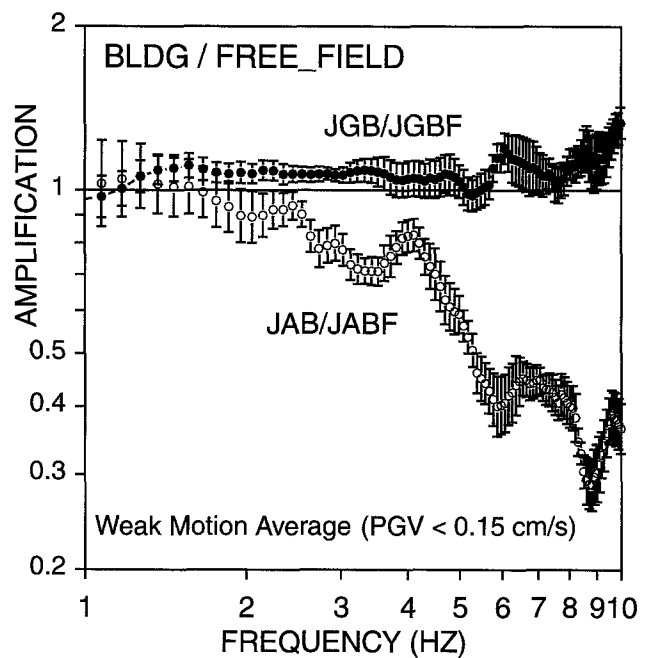


Figure 6. Geometric mean of the spectral ratio of motion recorded inside and outside the administration building (JAB/JABF) and the generator building (JGB/JGBF). The error bars represent plus and minus one standard deviation of the mean for seven weak-motion events (PGV at JGB less than 0.15 cm/sec) recorded on the portable GEOS instruments.

5 shows the velocity time series of a weak-motion event recorded inside and outside the two buildings. The motion recorded at JAB is lacking high-frequency ground motion compared with the free-field site (JABF). The JGB instrument, on the other hand, recorded a signal very similar to that of JGBF, though there is a slight difference in amplitude. These time-domain differences show up clearly in the geometric average of the spectral ratios inside and outside the structure (Figure 6). The differences in the building/free-field response between the two sites is dramatic: the average spectral ratio between the basement of the administration building and the free-field site (JAB/JABF) decreases strongly with frequency beginning at 2.5 Hz, but the data from the generator building station shows a relatively constant, small amplification relative to the free-field site (JGB/

JGBF). To unravel the various effects of embedment depth, soil-structure interaction, and the averaging of motions over the horizontal dimensions of the structures, plans are currently underway by C.B. Crouse (personal comm., 1998) to vibrate the structures and analyze the response using computer modeling (as Crouse and Hushmand, 1989, did in studying the effect of the structure housing an accelerometer in the Imperial Valley, California).

Spectral Ratios of the Accelerograph Data

The main purpose of our study is to evaluate the dependence of the spectral amplitudes at the softer site on the level of the ground shaking at the reference site. Unfortunately, the larger-amplitude data were recorded inside the buildings only; free-field recordings are available for seven of the

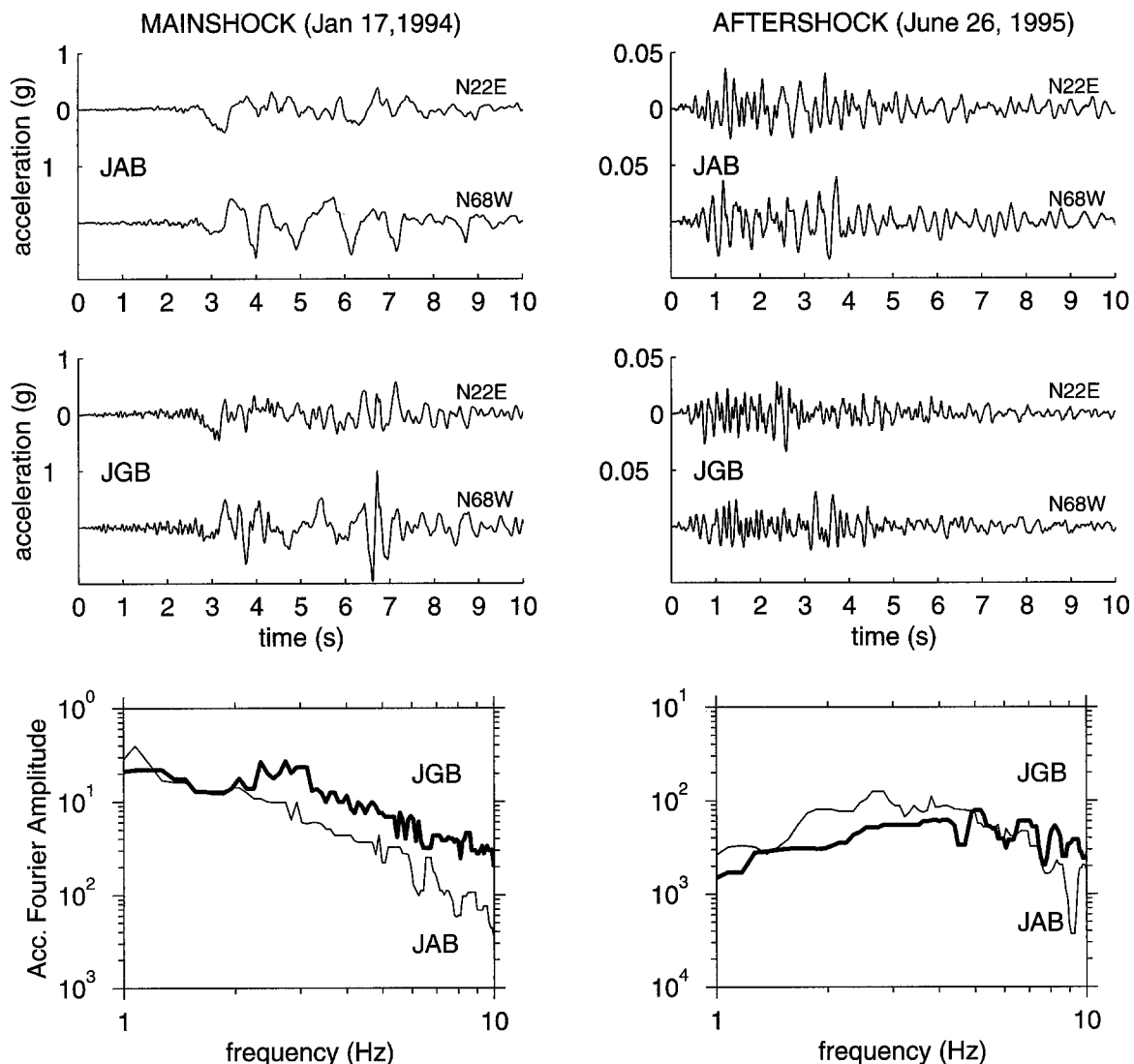


Figure 7. Horizontal accelerations (N22E and N68W directions) recorded at JAB and JGB SMA-1 stations during the 1994 Northridge mainshock and for a weak-motion aftershock occurring on 26 June 1995. The figure shows the average of the Fourier amplitude spectra for the two horizontal components in $[g \text{ sec}]$ units; thin line, JAB; thick line, JGB.

events, but the motions for these recordings are very small (see the peak velocities in Table 3). We showed in the previous section that the recordings in the structures can be very different from the nearby free-field recordings, particularly at JAB. In order to remove the imprint of the structures on the data, we decided to correct the Fourier spectra of the SMA-1 accelerations from within the buildings by using the average building/free-field spectral ratios obtained with the GEOS data. Several considerations allowed us to use those ratios as correction factors for the observed spectra at the two buildings, particularly (1) the sensor-mass release test on the GEOS instruments shows that their calibration responses are very similar, and (2) we collected enough event recordings to have a stable average. In applying these correction functions, which were computed from weak-motion data, to the strong-motion accelerograms, we implicitly assume that the effect of the buildings on the ground motion is not strongly dependent on the amplitude of the motion. Some justification for this assumption is that even for very weak motions, the administration building shows a large structure effect. In the following analysis, we approximated the free-field spectral ratio that would have been obtained from sites outside the buildings by multiplying the observed spectral ratios JAB/JGB from SMA-1 records by the frequency-dependent curve $(JGB/JGBF)/(JAB/JABF)$, where $(JGB/JGBF)$ and $(JAB/JABF)$ are geometric averages of the ratios from the seven events recorded on the GEOS units.

Mainshock and Later Aftershocks Figure 7 shows the horizontal time series and average Fourier amplitude spectra recorded at both stations for the 1994 Northridge mainshock and for a small event in 1995. The most evident characteristic on the records is the deficiency of high frequencies at JAB, particularly for the mainshock. In Figure 8, we compare the corrected spectral ratios of the two largest events (the 1994 Northridge mainshock, $M = 6.7$ and the 1994 March 20 aftershock, $M = 5.3$) with the corrected geometric average of spectral ratios of weak-motion events 2 through 11 (Table 3) recorded from 1995 to 1998 at SMA-1 and GEOS stations. The geometric average of the peak ground acceleration on the two horizontal components at JGB is 0.75 g for the mainshock, 0.22 g for the 1994 aftershock, and less than 0.032 g for the small aftershocks. The relative site response is strongly dependent on the amplitude of the motion. The amplifications of the mainshock and the 20 March 1994 event are similar and significantly smaller than those for the weak-motion events for frequencies greater than about 2.5 Hz. Even without correction for the building/free-field response factor, the relative differences in the JAB/JGB ratios between strong and weak motion would be the same, indicating the soil response is a function of the strength of ground shaking.

Immediate Aftershocks We refer to aftershocks AS1 through AS4 (Table 3) as "immediate" aftershocks because they occurred within two minutes of the mainshock. We also

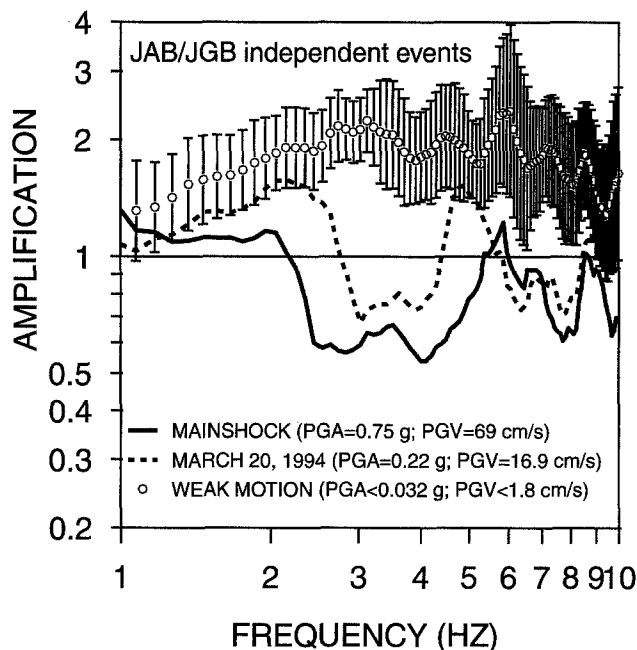


Figure 8. Spectral ratios (JAB/JGB) corrected for the effect of the structure in which the recordings were made, of the mainshock, March 20 aftershock, and geometric average of the independent weak-motion recordings. We computed the PGA and PGV values as the geometric mean of the maximum peaks in the two horizontal directions at JGB. The small amplitude signals (ten events) have been recorded from 1995 to 1998 at SMA-1 (three events) and GEOS stations (seven events) inside the two Jensen buildings (JAB, JGB) and the error bars were derived by combining the standard deviation of the observations about the mean spectral ratio of the weak-motion events (events 2–11 in Table 3) and the uncertainty in the free-field/building effect.

include AS6 and AS7 in this grouping, although they occurred eleven to twelve hours after the mainshock (AS5 was not recorded at JAB and JGB). The peak ground-motion values at JGB for these aftershocks range from 0.13 g (for AS1) to 0.016 g (for AS4). Figure 9 shows the corrected spectral ratios computed for the immediate aftershocks and, for comparison, the average spectral ratio of the weak-motion aftershocks occurring several years after the mainshock (this ratio is referred to as the weak-motion average in the figures). Also shown is the ratio of the mainshock motions. (The spectra of the immediate aftershocks will be influenced by the coda of the mainshock, particularly at low frequencies; what is important is that we are extracting low-amplitude motions for comparison with the stronger motions.) For frequencies between about 2 and 4 Hz, the ratios of the smaller immediate aftershocks (AS2, AS4, and AS6) are similar to those for the later weak motions and differ from the larger immediate aftershocks (AS1, AS3, and AS7). Whether this difference is meaningful is uncertain. More importantly, the high-frequency ratios (above about 4 Hz) for

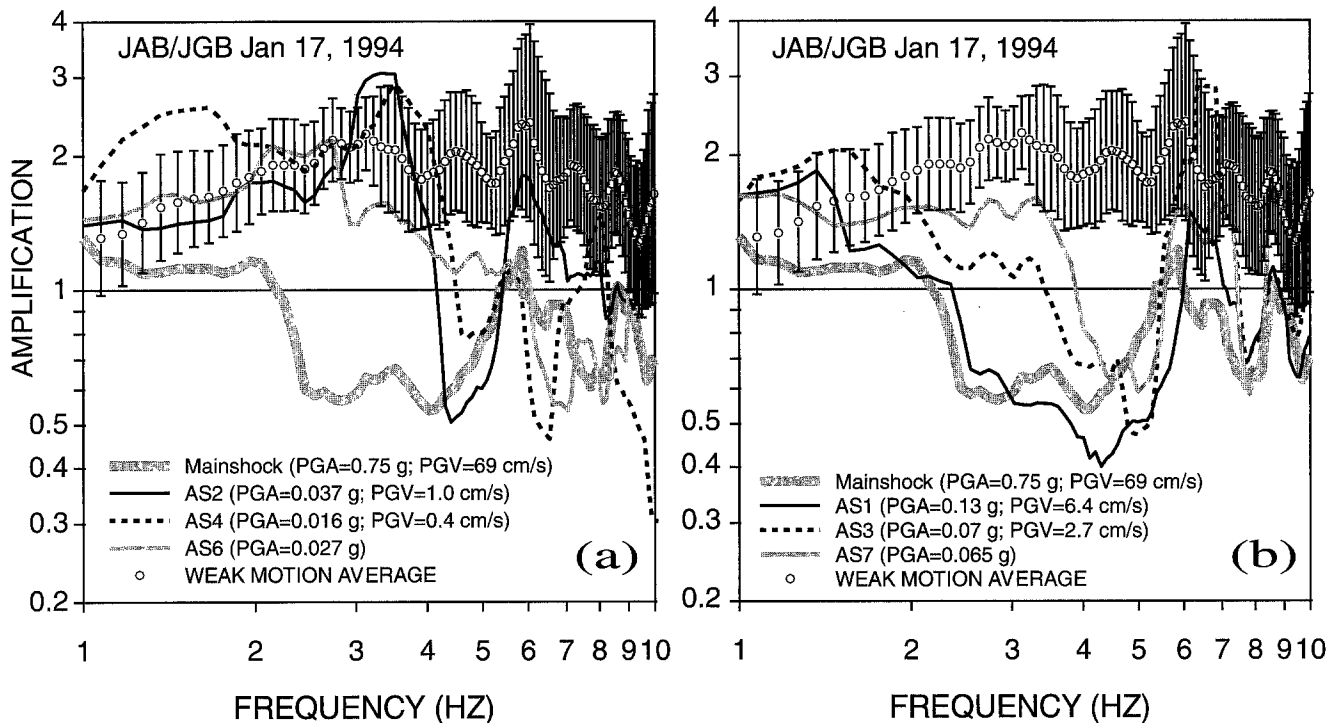


Figure 9. Comparison between the corrected spectral ratios of six immediate aftershocks (most within three minutes of the mainshock) and the corrected average of the independent weak-motion recordings at the Jensen stations (the error bars show the standard deviation of the observations about the average spectral ratio and include the uncertainty of the free-field/building correction). The ratios have been corrected for the effect of the structure in which the recordings were made. To facilitate the comparison, the smaller and larger immediate aftershocks are shown separately in parts (a) and (b). All peak motions are for JGB; see Figure 8 caption.

all of the immediate aftershocks are very different from the ratios of the later aftershocks and are similar to the mainshock ratio despite the relatively small-amplitude motions of the immediate aftershocks. As we discuss later, the apparent difference of the ratios of small-amplitude motions according to whether the motions were obtained immediately after the mainshock or at a later time may be explained by an increase in pore pressure during the mainshock strong shaking that did not dissipate for hours.

Coda Waves To augment the motions from individual events, we computed spectral ratios of the horizontal motion from coda waves of the larger events. We defined the coda as the portion of the *S*-wave starting after the shaking dropped to less than about 20% of the peak acceleration. Figure 10a shows the ratios for the mainshock coda, the coda of the two larger immediate aftershocks, and for comparison, the ratio of the *S*-wave portion of the mainshock. In spite of the large difference in amplitudes (peak accelerations ranging from 0.016 to 0.75 *g*), the spectral ratios of the motions within the first two minutes of the mainshock are all similar (ratios of the *S*-wave portions of the immediate aftershocks are shown in Figure 9 and to avoid clutter have not been included in Figure 10a). In contrast, Figure 10b shows that

the ratios of coda amplitudes for the 20 March 1994 and 26 June 1995 aftershocks are similar to the ratios of the *S*-wave portions of the ten weak-motion events that we use as a reference, even though the amplitudes of the codas are similar to those of the codas of the immediate aftershocks. The ratio of the coda for the March 20 event differs significantly from the ratio of *S*-wave portion of the March 20 earthquake (Figure 8).

Discussion To summarize, the spectral ratios from the mainshock and their coda, the immediate aftershocks and their coda, and the large aftershock on 20 March 1994 all show a deficiency of high-frequency motion at JAB relative to JGB that is not seen in the spectral ratios of the weak-motion aftershocks occurring several years later. We consider the differences in the ratios of strong shaking and the weak-motion average to be direct evidence for nonlinear response of the soils. In a later section, predictions based on conventional engineering practice indicate that the nonlinearity is occurring at shallow depths, primarily between 9 and 15 m. A question is whether the nonlinearity would be the same in the absence of the structure, or whether some property of the structure or its response modified the nonlinear soil response. We have no way answering this question, but

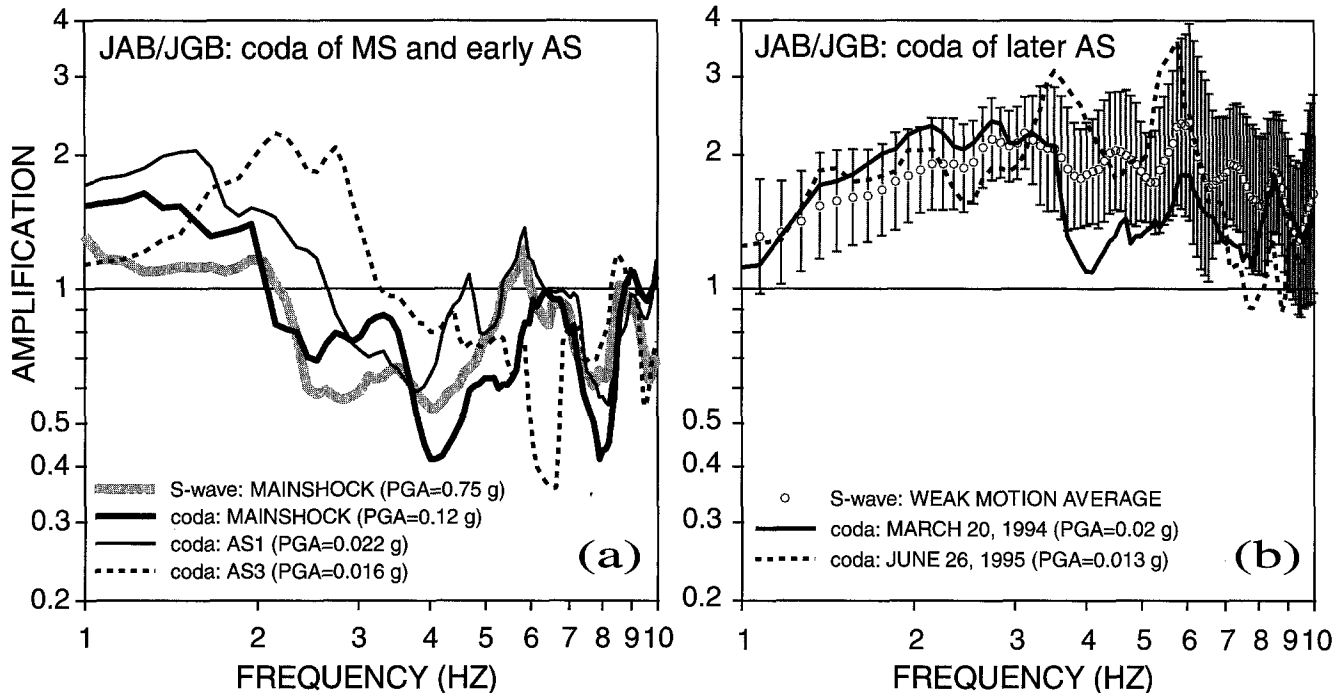


Figure 10. Coda-wave spectral ratios: (a) for the larger events on 17 January 1994; (b) for independent events. For comparison, (a) contains the ratio of the *S*-wave portion of the mainshock, and (b) contains the weak-motion average (the error bars show plus and minus one standard deviation of the observations about the average spectral ratio and include the uncertainty of the free-field/building correction). The ratios have been corrected for the effect of the structure in which the recordings were made. All peak motions are for JGB; see Figure 8 caption.

we will maintain the portable instruments in the field as long as possible, hoping that they will record a motion large enough to assess whether the nonlinear response is identical at the free-field sites and the building sites.

Analysis of Data from Rinaldi and Los Angeles Dam

The second pair of sites we analyzed (RIN and LAD) are installed south of the JFP in free-field locations; unlike the case for the Jensen plant recordings, we do not have to make corrections for the effect of structure in which the recorder is housed. The distance between the two stations is 1.5 km (Figure 2), and the difference in the *S*-wave velocity model at the two sites is greater than for the Jensen stations (Figure 4). Because of the greater distance between the stations, the assumption that the spectral ratio is a direct estimate of the relative site response between the two stations is less certain than it is for the Jensen stations. The deepest parts of the boreholes penetrated different geologic units, although the ages and velocities of these units are similar (Figure 4). In the calculation of spectral ratios, we chose LAD as a reference site because it would be classified as a rock site based on the geologic description of the borehole cuttings (see Gibbs *et al.*, 1996). This description is consistent with the shear-wave velocities beneath the site ($V_{30} = 647$ m/sec,

compared with 620 m/sec for an average rock site, according to Boore and Joyner, 1997). It should be noted, however, that the measurement of $D = 8\%$ indicates strong attenuation in the upper 90 m. As we will see, this large attenuation will influence the level of the spectral ratios (with the spectra from LAD in the denominator).

The only data we have recorded at both RIN and LAD are the records of the mainshock and one aftershock occurring about ten minutes after the mainshock (AS5); we also used the coda waves of the mainshock motion as a surrogate for small amplitude earthquake recordings. Time series and spectra for the mainshock recorded at RIN and LAD are shown in Figure 11. The largest ground-motion velocity ever recorded from an earthquake (over 170 cm/sec on one horizontal component) was derived from the accelerograph recording at RIN (the geometric average of the two horizontal components is 114 cm/sec). The spectrum for the motion at RIN suggests the presence of three peaks at 1, 3, and near 5 Hz, which is close to the sequence of frequencies expected for resonance in a layer over a halfspace. If the peaks are due to resonances in site response, it might be expected that the frequencies of these peaks would be a function of amplitude of shaking because of changes in shear-wave velocity resulting from nonlinear soil response. We found no consistent patterns in the peaks of the motions. Anticipating the

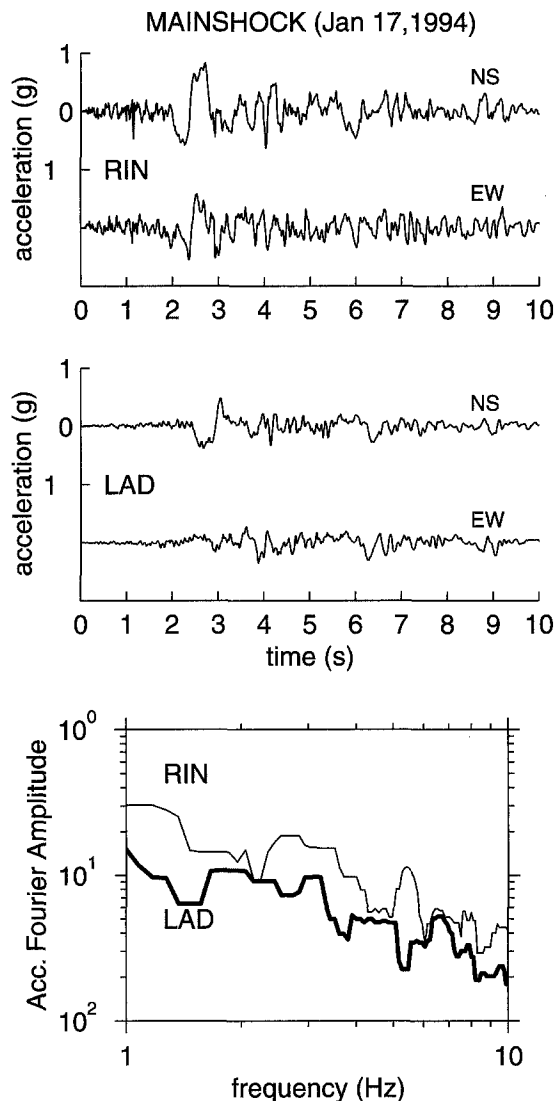


Figure 11. Horizontal accelerations (N-S and E-W directions) recorded at RIN and LAD SMA-1 stations during the 1994 Northridge mainshock. The figure shows the horizontal average amplitude Fourier spectra of these records in $[g \text{ sec}]$ units, with thin line for RIN and thick line for LAD.

result, we do not think that a convincing case for nonlinear soil response can be made from the peaks in the spectral ratios; on the other hand, differences in the overall levels of the RIN/LAD spectral ratio for the mainshock, the mainshock coda, and AS5 are probably an indication of soil nonlinearity.

Mainshock and Weak-Motion Spectral Ratios

The spectral ratios for the mainshock *S*-wave, a portion of the coda following the *S*-wave, and AS5 are shown in Figure 12. The mainshock motion at RIN relative to the ground shaking recorded at LAD is amplified by factors ranging from 1.1 to 3 for frequencies higher than 1 Hz, with three peaks in the frequency range of 1 to 6 Hz. The spectral

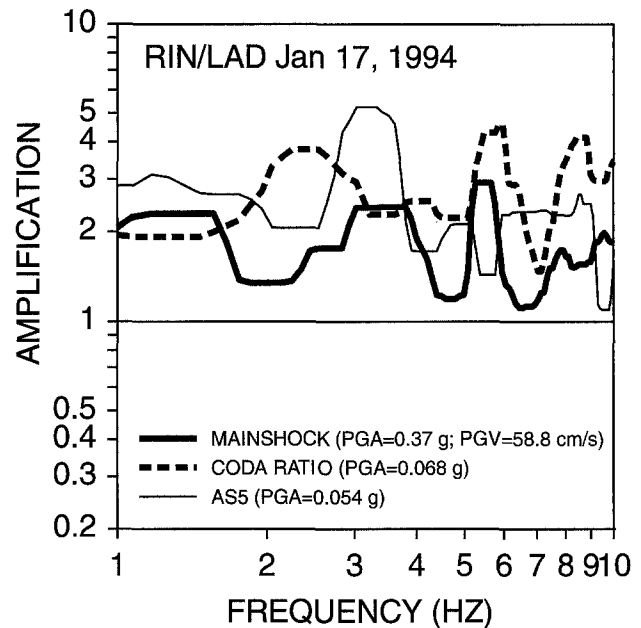


Figure 12. Horizontal spectral ratios of motions recorded at RIN and LAD, including the mainshock, coda waves of the mainshock, and an aftershock occurring about 10 min after the mainshock. The PGA values are the geometric means of the two horizontal components at LAD.

ratios for the coda waves and AS5 are generally larger than those for the mainshock, unlike the case for the Jensen recordings, for which the mainshock ratios, aftershock ratios, and coda ratios were similar (e.g., Figures 9 and 10a). The coda and AS5 ratios have spectral peaks, but they occur at different frequencies from each other and from the peaks in the mainshock ratio. We think it is difficult to relate these peaks to those in the mainshock spectral ratio, and moreover, as shown later they do not agree in location with predictions using the shear-wave velocities from the boreholes. The important observation is the overall difference in spectral ratio between the mainshock and the weaker amplitude coda and AS5 motions. We consider this to be an indication of soil nonlinearity. In the next main section we will compare the observations with predictions using conventional engineering practice for accounting for soil nonlinearity.

Horizontal to Vertical Spectral Ratio

Some authors have found that the ratio of horizontal to vertical motion (H/V) can be used to identify site resonances, at least for the resonant peak of the fundamental mode (e.g., Lermo and Chavez-Garcia, 1993; Field and Jacob, 1995; Bonilla *et al.*, 1997). Shifts in the frequencies of the resonance modes as a function of amplitude of shaking might be an indication of soil nonlinearity. We show the H/V spectral ratios at RIN and LAD for the mainshock, coda, and AS5 in Figure 13. The H/V for the mainshock has peaks near 1, 2.8, and 5.5 Hz, which are grossly similar to those in the RIN/

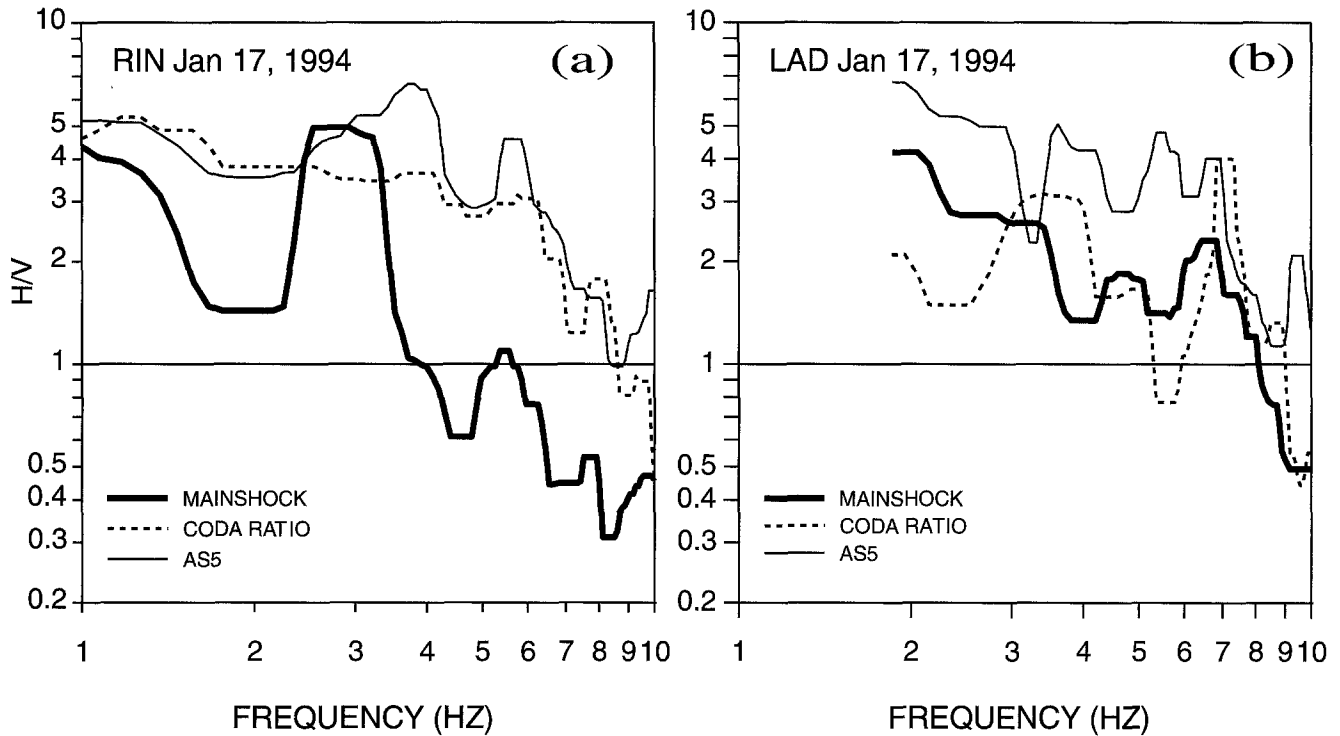


Figure 13. Ratios of horizontal-component to vertical-component Fourier amplitude spectra at RIN and LAD for the mainshock, the coda of the mainshock, and an aftershock occurring about 10 min after the mainshock. A limited frequency range is shown for LAD because the AS5 data were filtered at 1.8 Hz on the vertical component.

LAD ratio for the mainshock. The comparison, however, is not very certain. The more obvious feature in Figure 13 is the large difference in H/V between the mainshock and the weaker motions at station RIN (similar differences are not seen at LAD). We do not know if the difference is related to soil nonlinearity or to some other factors that are not amplitude-dependent (such as radiation pattern or source finiteness). We show H/V more for completeness of the analysis than because we can use it in an argument for or against nonlinearity of soil response; the dependence of the RIN/LAD ratio is a more direct indication of soil nonlinearity.

Comparison of the Spectral Ratios with Predictions of Soil Response using Conventional Engineering Practice

The data analysis in the previous sections showed that the spectral ratios depend on the amplitude of the ground shaking. The most obvious explanation for this behavior is nonlinear soil response. In this section, we follow conventional engineering practice to simulate the effects of soil nonlinearity on the spectral ratios; we compare the simulated ratios to the observed ratios.

The Computation of Nonlinear Response

Conventional engineering practice for the simulation of nonlinear soil response uses the equivalent linear method, as

implemented by the program SHAKE91 (Schnabel *et al.*, 1972, Idriss and Sun, 1992). We follow that practice in our simulations. The equivalent linear method is based on the assumption that the soil response can be approximated by a linear viscoelastic model, whose properties (shear modulus and damping) are chosen in accord with the average strain occurring at the middle of each soil layer. Given the time series at the base of the stack of soil layers, the response of the system to vertically propagating shear waves is calculated. The computer program requires a time series as input motion and curves describing the strain-dependence of shear modulus and damping at various depths. We used two different sets of shear modulus and damping ratio curves. One is included in the sample input for the SHAKE91 program (Idriss and Sun, 1992, Table 1), and the other was recommended to us by W. Silva as being appropriate for our application (W. Silva, personal comm., 1997). We modified the low-strain damping using the measured values from Table 2, and we used the borehole velocity profiles in Figure 4 to define the low-strain values of the shear modulus. The theoretical spectral ratios (JAB/JGB) obtained with the two sets of modulus reduction and damping curves were very similar and, for simplicity, for comparison with data we decided to use only the curves included in the sample input for the SHAKE91 program.

The SHAKE91 program requires the specification of a time series as input at the base of the soil layers. This is

often taken as the surface motion at the reference site. As pointed out by a number of authors (e.g., Steidl *et al.*, 1996, and Boore and Joyner, 1997), however, this procedure is incorrect: it is important to remove the response of the reference site, even if the site is underlain by rock. We did this by using an option in SHAKE91 to deconvolve the observed surface motions to obtain the motions at the bottoms of the reference site boreholes (JGB and LAD). This gave motions at the bottom that are consistent with any nonlinear response included in the SHAKE91 calculations. We used these deconvolved reference-site motions as input to the soil columns under the other pair of stations (i.e., deconvolved JGB and LAD as input to JAB and RIN, respectively). Surface motions were calculated for each of the two horizontal components of input motion. We treated these in the same way as we did the observed time series, computing spectral ratios (JAB/JGB and RIN/LAD) of the averaged horizontal components. In these ratios, the actual surface motions at the reference sites, rather than the deconvolved motions, were used in the denominators; the deconvolved motions were only used as input at the base of the numerator sites (we verified that convolving the deconvolved records returned the surface motions). All of our calculations assume horizontally stratified layers and vertical incidence; runs with a purely linear model for angles of incidence up to 40 degrees gave results similar to vertical incidence.

To emphasize the dependence of the soil response on the amplitude of the input motion, we present ratios of the relative site response (e.g., JAB/JGB) computed for strong shaking and for weak shaking. The advantage of using ratios of ratios is that it isolates the relative changes due to nonlinearity; even if the computed relative-site responses are not computed exactly because of differences between reality and our models (due, for example, to lateral heterogeneities in soil properties), we expect that relative changes in the ratios as a function of soil amplitude will not be sensitive to these inadequacies in the soil model.

Comparison of Simulated and Observed Amplitude-Dependence

In Figure 14 we compare the ratio of spectral ratios (that is, JAB/JGB for strong motion divided by the average JAB/JGB ratio for weak motions) for the simulations and for the two largest earthquakes recorded at the Jensen sites. The observed and simulated ratios for the mainshock are somewhat similar in shape. Perhaps most significant is the agreement of the reductions in amplitude (by factors of 0.2–0.6) for frequencies above about 4 Hz. The comparison between observations and simulations for the March 20 event is not nearly so good, with the observations indicating more nonlinearity than predicted by the theory. Both the observations and the simulations, however, show reductions in amplitude for frequencies greater than about 4 Hz. The comparisons shown in Figure 14 suggest that a significant portion of the relative soil response of the two sites can be explained by standard equivalent-linear models.

JAB/JGB observations & theory: large/weak

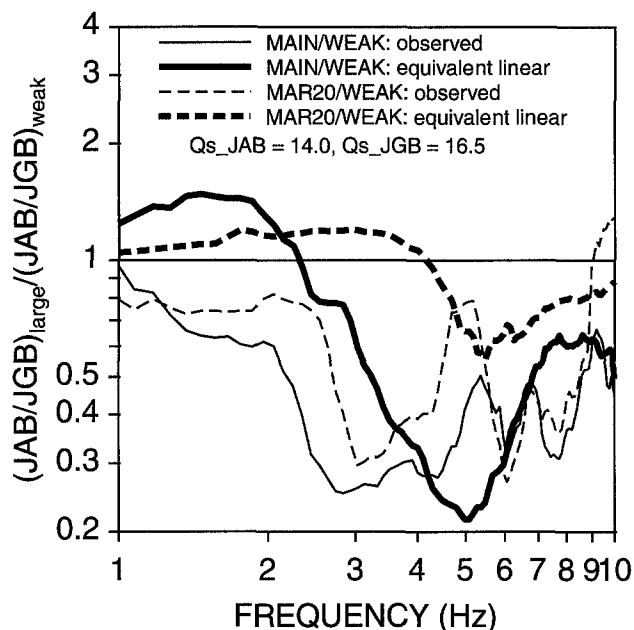


Figure 14. Ratios of relative site response at JAB/JGB for large events (mainshock and March 20 aftershock) and weak-amplitude motions. Comparison between the observed data and the theoretical computations from the equivalent linear method (SHAKE91 code).

Recall that the JAB/JGB spectral ratios for the weak-amplitude motions immediately following the mainshock are similar to the ratio of mainshock spectra (Figures 9 and 10a). In contrast, the predicted ratio of spectral ratios for the small aftershocks are essentially equal to unity (we did the computations for the 26 June 1995 aftershock with $PGA = 0.032$ g, but for clarity did not plot the results in Figure 14). An explanation for this difference in observed and predicted dependence of the spectral ratios on amplitude of shaking might be that pore pressure increased as a result of the strong shaking, causing changes in the properties of the soil that persisted for at least the following twelve hours. The persistence of excess pore pressure during the mainshock could explain the differences in site response for the immediate aftershocks and for the coda waves. A recent study of liquefaction, observed with a vertical array during the 1995 Kobe earthquake (Aguirre and Irikura, 1997), shows that the change of soil rigidity gradually recovers with time and the liquefied state remains at least 3 hr after the mainshock but no more than 24 hr. Similar behavior was observed during the 1987 Superstition Hills earthquake (Holzer *et al.*, 1989). The existence of elevated pore pressure at the Jensen Filtration Plant is suggested by lateral displacements observed near JAB, although we cannot be sure that liquefaction occurred because no sand boils were observed at the surface of the site (Stewart *et al.*, 1996).

The comparison of the simulated and observed re-

sponses for RIN/LAD are shown in Figure 15. Because we do not have a well determined estimate of the low-amplitude ratios, we cannot compute a ratio of spectral ratios, as we did for the Jensen recordings. In this case, the figure shows the spectral ratios themselves. The spectral ratios for both the linear and equivalent-linear models and the observations are greater than unity. (The linear calculations were done using C. Mueller's program RATTLE and are based on the Thomson-Haskell method.) The theoretical ratios are controlled both by amplifications at RIN and by a reduction of the high-frequency amplification at the reference site (LAD) caused by the large low-strain damping at that site ($D = 8\%$). (The high-frequency amplification for the linear model is about 1.5 times higher than it would be if no attenuation were included.)

Both the purely linear and the equivalent-linear calculations match the overall observed level of the spectral ratio for frequencies less than about 4 Hz. For higher frequencies, however, the observed response lies between the purely linear and the equivalent-linear responses. Based on this comparison, we conclude that the soil response was not quite as nonlinear at RIN as predicted by standard engineering practice.

Of interest in the understanding the results are the layers in which most of the nonlinearity occurs. This information is part of the output of program SHAKE91. At JAB, most of the nonlinearity occurred at depths between 9 to 15 m. The low shear modulus in this depth range (see Figure 4) pro-

duced a very large concentration of strain compared with the other layers (more than 10 times higher). Even though the shear-wave velocities beneath RIN are generally lower than those at JAB, the strain concentration beneath RIN was not as great as at JAB, being about 3 times higher than in other layers for depths between 6 to 13 meters. Therefore, the nonlinearity of the response was not as great. The difference in strain is understandable in terms of the details of the velocity profiles (Figure 4): the velocity is smaller at RIN near the surface, but shear strain must go to 0.0 near the surface, so the low near-surface velocity at RIN does not lead to a strain concentration. In contrast, the low velocity fluvial terrace deposits at JAB are sandwiched between the higher velocity engineered fill above and the Saugus formation below at a sufficient depth that significant strain concentrations can occur.

Our goal in this section was simply to compare the observed soil response with that computed using conventional engineering practice. We have made no attempt to provide a quantitative assessment of the discrepancies between the simulated and observed responses. This would require estimates of the uncertainty in the equivalent linear calculations due to variations in the soil properties, the input motion, and the model of nonlinear response (plane layers, vertical propagation, equivalent linear analysis).

Conclusions

We have shown that the spectral ratios of motions at two pairs of sites in the VNC on the edge of the San Fernando Valley in California are dependent on the amplitude of the shaking. At the JFP, the spectral ratio for site JAB relative to JGB for the mainshock was as much as a factor of 0.3 smaller than the ratio for low-strain motions, indicating substantial nonlinear response of the soils. The amplitude dependence of the ratios is in general agreement with equivalent linear calculations using conventional engineering practice and low-strain properties measured at the sites. One exception to the amplitude dependence of the ratios were the ratios for small motions within the first twelve hours after the mainshock; at high frequencies these motions have similar spectral ratios to that of the mainshock. The difference in behavior of these low-strain motions immediately after the mainshock and motions recorded months to years after the mainshock may be due to the persistence of increases in pore pressure at JAB that originated during the mainshock.

Using recordings of small earthquakes on portable seismographs installed almost four years after the mainshock, we conclude that the motions of the permanently-installed accelerometers that recorded the mainshock and a number of aftershocks are influenced by the buildings in which the instruments are housed. The effect is particularly noticeable at station JAB, for which the high-frequency motions are reduced to less than 0.4 of those at a nearby free-field site. This strong building effect does not impact our conclusions about soil nonlinearity, for we use the relative change in

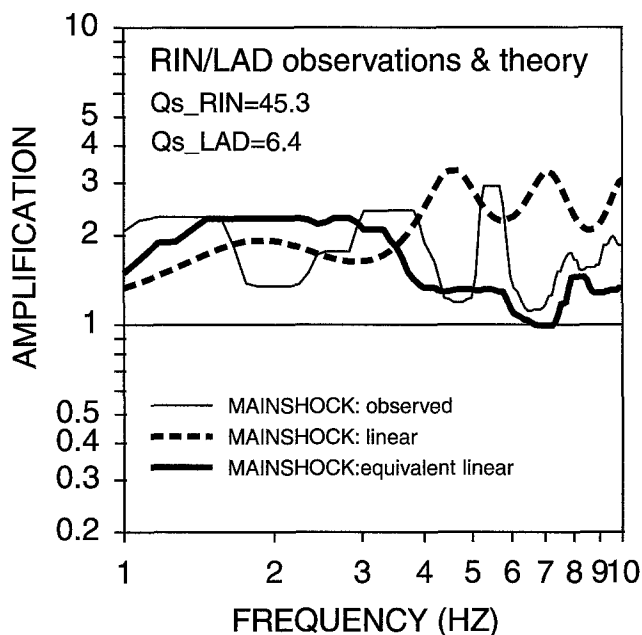


Figure 15. Comparison between the observed and theoretical spectral ratios (RIN/LAD) for the 1994 Northridge earthquake. We computed the transfer functions at the two sites using purely linear calculations (program RATTLE) and equivalent linear calculations (program SHAKE91).

ratios as a function of amplitude of ground motion for a suite of recordings made on the same instruments. It does impact to some extent many of the studies that used the JAB mainshock record and the weak-motion aftershock recording from the U.C. Santa Barbara station located outside of (not colocated with) JAB in their search for soil nonlinearity during the 1994 Northridge earthquake; this includes Trifunac and Todorovska (1996), Field *et al.* (1997, 1998), Beresnev *et al.* (1998a), and Su *et al.* (1998). Fortunately, these studies used data from many soil sites, so the impact of including JAB would be strongly diluted.

At the Rinaldi Receiving Station, our data are not as complete as at the Jensen plant, but we again find evidence for nonlinear soil response during the mainshock. The spectral amplitudes at the soil site (RIN) are elevated relative to those at the rock site (LAD) for all frequencies studied in this paper (1–10 Hz). This is probably due to a combination of site amplification at RIN and the large amount of shear-wave damping at the reference site (LAD). The observed ratio for the mainshock falls between the predictions from the linear and equivalent linear models, suggesting that the degree of nonlinearity is somewhat smaller than predicted by standard practice.

Acknowledgments

We owe thanks to many people who helped us in this research: Craig Davis and Ron Tognazzini of the LADWP for data, discussions, and a tour of the sites; George Barker, Douglas Cox, and David Dean of the MWD for assistance in the deployment of the portable GEOS recorders at the Jensen Filtration Plant; Jack Boatwright and Walt Silva for providing a number of useful suggestions; Walt Silva for a set of modulus reduction and damping ratio curves; John Tinsley for sharing his knowledge of the geology of the area; Jim Gibbs for providing his measurements of attenuation in advance of publication; C. B. Crouse for giving us advice regarding the influence of the buildings on the recorded motions and prodding us into mounting the field experiment with the portable recorders; Ron Porcella for information about the strong-motion recordings at the Jensen plant; Chris Stephens for help in digitizing the film records; and Fabian Bonilla, Ken Campbell, Rob Kayen, Paul Spudich, Maria Todorovska, and an anonymous reviewer for thoughtful comments on the manuscript. We also thank Maria Todorovska for aftershock data. This project was initiated by G. Cultrera while she was visiting the USGS on an overseas fellowship from the University of Palermo, Italy.

References

- Aguirre, J., and K. Irikura (1997). Nonlinearity, liquefaction, and velocity variation of soft soil layers in Port Island, Kobe, during the Hyogoken Nanbu earthquake, *Bull. Seism. Soc. Am.* **87**, 1244–1258.
- Anderson, J. G., and S. E. Hough (1984). A model for the shape of the Fourier amplitude spectrum of acceleration at high frequencies, *Bull. Seism. Soc. Am.* **74**, 1969–1993.
- Bardet, J. P., and C. Davis (1996a). Engineering observations on ground motion at the Van Norman Complex after the 1994 Northridge Earthquake, *Bull. Seism. Soc. Am.* **86**, S333–S349.
- Bardet, J. P., and C. Davis (1996b). Performance of the San Fernando Dams during the 1994 Northridge earthquake, *J. Geotech. Eng. Div., ASCE*, **122**, 7.
- Bardet, J. P., and C. Davis (1996c). Performance of the two reservoirs during the 1994 Northridge earthquake, *J. Geotech. Eng. Div., ASCE*, **122**, 8.
- Beresnev, I. A., G. M. Atkinson, P. A. Johnson, and E. H. Field (1998a). Stochastic finite-fault modeling of ground motions from the 1994 Northridge, California earthquake. II. Widespread nonlinear response at soil sites, *Bull. Seism. Soc. Am.* **88**, 1402–1410.
- Beresnev, I. A., E. H. Field, K. Van Den Abeele, and P. A. Johnson (1998b). Magnitude of nonlinear sediment response in Los Angeles basin during the 1994 Northridge, California, earthquake, *Bull. Seism. Soc. Am.* **88**, 1079–1084.
- Bonilla, L. F., J. H. Steidl, G. T. Lindley, A. G. Tumarkin, and R. J. Archuleta (1997). Site amplification in the San Fernando Valley, California: variability of site-effect estimation using the *S*-wave, coda, and H/V methods, *Bull. Seism. Soc. Am.* **87**, 710–730.
- Boore, D. M., and W. B. Joyner (1997). Site-amplifications for generic rock sites, *Bull. Seism. Soc. Am.* **87**, 327–341.
- Borcherdt, R. D., J. B. Fletcher, E. G. Jensen, G. L. Maxwell, J. R. Van Schaak, R. E. Warrick, E. Cranswick, M. J. S. Johnston, and R. McClearn (1985). A general earthquake-observation system, *Bull. Seism. Soc. Am.* **75**, 1783–1825.
- Crouse, C. B., and B. Hushmand (1989). Soil-structure interaction at CDMG and USGS accelerograph stations, *Bull. Seism. Soc. Am.* **79**, 1–14.
- Electric Power Research Institute (EPRI) (1993). Guidelines for determining design basis ground motions, Electric Power Research Institute, Palo Alto, California, Rept. No. EPRI TR-102293.
- Field, E. H., and K. H. Jacob (1995). A comparison and test of various site-response estimation techniques, including three that are not reference-site dependent, *Bull. Seism. Soc. Am.* **85**, 1127–1143.
- Field, E. H., P. A. Johnson, I. A. Beresnev, and Y. Zeng (1997). Nonlinear ground-motion amplification by sediments during the 1994 Northridge earthquake, *Nature* **390**, 599–602.
- Field, E. H., Y. Zeng, P. A. Johnson, and I. A. Beresnev (1998). Nonlinear sediment response during the 1994 Northridge earthquake: observations and finite-source simulations, *J. Geophys. Res.* **103**, 26,869–26,883.
- Gibbs, J. F., D. M. Boore, W. B. Joyner, and T. E. Fumal (1994). The attenuation of seismic shear waves in Quaternary alluvium in Santa Clara Valley, California, *Bull. Seism. Soc. Am.* **84**, 76–90.
- Gibbs, J. F., J. C. Tinsley, and W. B. Joyner (1996). Seismic velocities and geologic conditions at twelve sites subjected to strong ground motion in the 1994 Northridge, California earthquake, *U. S. Geol. Surv. Open-File Rept. 96-740*, 103 pp.
- Hartzell, S. (1998). Variability in nonlinear sediment response during the 1994 Northridge, California, earthquake, *Bull. Seism. Soc. Am.* **88**, 1426–1437.
- Heaton, T. H., J. F. Hall, E. H. Field, and M. W. Halling (1995). Response of high-rise and base-isolated buildings to a hypothetical M_w 7.0 blind thrust earthquake, *Science* **267**, 206–211.
- Holzer, T. L., T. L. Youd, and T. C. Hanks (1989). Dynamics of liquefaction during the 1987 Superstition Hills, California, earthquake, *Science* **244**, 56–59.
- Idriss, I. M., and J. I. Sun (1992). User's Manual for SHAKE91. Center for Geotechnical Modeling, Dept. of Civil and Environmental Engineering, U. of California, Davis.
- Lermo, J., and F. J. Chavez-Garcia (1993). Site-effect evaluation using spectral ratios with only one station, *Bull. Seism. Soc. Am.* **83**, 1574–1594.
- Lindvall-Richter-Benuska Associates (1994). Processed LADWP power system strong-motion records from the Northridge, California earthquake of January 17, 1994a, report prepared for Los Angeles Department of Water and Power, LRB No. 007-027, 165 pp.
- O'Rourke, T. D., B. L. Roth, and M. Hamada (1992). Large ground deformations and their effects on lifeline facilities: 1971 San Fernando earthquake, in *Case Studies of Liquefaction and Lifeline Performance During Past Earthquakes*, T. D. O'Rourke and M. Hamada (Editors) National Center for Earthquake Engineering Research, Buffalo, New York, Report NCEER-92-0002, 3-iii–3-85.

- Schnabel, P., H. B. Seed, and J. Lysmer (1972). Modification of seismograph records for effects of local soil conditions, *Bull. Seism. Soc. Am.* **62**, 1649–1664.
- Scientists of the U.S. Geological Survey and the Southern California Earthquake Center (1994). The magnitude 6.7 Northridge, California, earthquake of January 17, 1994, *Science* **266**, 389–397.
- Steidl, J. H., A. G. Tumarkin, and R. J. Archuleta (1996). What is a reference site? *Bull. Seism. Soc. Am.* **86**, 1733–1748.
- Stewart, J. P., R. B. Seed, and J. D. Bray (1996). Incidents of ground failure from the 1994 Northridge earthquake, *Bull. Seism. Soc. Am.* **86**, S300–S318.
- Su, F., J. G. Anderson, and Y. Zeng (1998). Study of weak and strong ground motion including nonlinearity from the Northridge, California, earthquake sequence, *Bull. Seism. Soc. Am.* **88**, 1411–1425.
- Trifunac, M. D., M. I. Todorovska, and S. S. Ivanovic (1994). A note on distribution of uncorrected peak ground accelerations during the Northridge, California, earthquake of 17 January 1994, *Soil Dyn Earthquake Eng.* **13**, 187–196.
- Trifunac, M. D., and M. I. Todorovska (1996). Nonlinear soil response—1994 Northridge, California, earthquake, *J. of Geotechnical Engineering* **122**, 725–735.
- Trifunac, M. D., M. I. Todorovska, and V. W. Lee (1998). The Rinaldi strong motion accelerogram of the Northridge, California earthquake of 17 January 1994, *Earthquake Spectra* **14**, 225–239.
- U. S. Geological Survey Home Page (1999). <http://nsmp.wn.usgs.gov/>.
- Wald, D. J., T. H. Heaton, and K. W. Hudnut (1996). The slip history of the 1994 Northridge, California, earthquake determined from strong-motion, teleseismic, GPS, and leveling data, *Bull. Seism. Soc. Am.* **86**, 49–70.
- Wang, L.-J., Q. Gu, and W. D. Iwan (1996). A collection of processed near field earthquake accelerograms with response and drift spectra, a report by Earthquake Engineering Research Laboratory, Calif. Institute of Technology, Pasadena, California, Report No. EERL 96-05, 141 pp.

Istituto Nazionale di Geofisica
Via di Vigna Murata 605
00143 Roma, Italy
E-mail: cultrera@ing750.ingrm.it
(G.C.)

U.S. Geological Survey, MS 977
345 Middlefield Road
Menlo Park, CA 94025
E-mail:
boore@usgs.gov
joyner@usgs.gov
dietel@usgs.gov
(D.M.B., W.B.J., C.M.D.)

Manuscript received 28 July 1998.